Understanding and Improving the Path of the Gulf Stream in Moderate Resolution Climate Models

End of First Year Report

Georgina Long
Supervisors: Prof. Beth Wingate & Dr. Mike Bell

May 2017

1 Introduction

Ocean eddies are the subject of many ongoing investigations into ocean dynamics. The topic comprises a broad range of smaller-scale dynamics and relationships at varying scales , with researchers are still trying to get a better understanding of the internal dynamics of the ocean. Our main focus will be on the area of the Gulf Stream and mainly the interaction and effect of the bathymetry on the separation and subsequent path of the Gulf Stream.

1.1 The impact of an accurately resolved Gulf Stream

The Gulf Stream is part of the AMOC and is essential to transferring heat from the Gulf of Mexico at lower latitudes towards western and northern Europe. Fundamentally it gives north-western Europe its mild climate and thus has large impacts on the weather as the heat is transferred into the atmosphere. This can have wide ranging effects on weather prediction such as winter blocking (Scaife *et al.*, 2011).

Variations in the Gulf Stream have also been linked to flooding on the U.S. east coast caused by the increase in sea surface level by (Ezer, 2015) among others.

It has been identified that the Gulf Stream has evolved over time, with (Greatbatch, Fanning, and Goulding, 1991) identifying a weakening of ∼30Sv between data from 1955-59 and 1970-74. The dependence on the Gulf Stream for weather gives greater importance to our understanding and ability to predict the changes in the Gulf Stream. Many lower resolution models render an unrealistic Gulf Stream, with the separation from the U.S. coast too far to the south, causing an inaccurate path from this point onwards. This causes knock-on effects as the corresponding sea surface temperatures (SSTs) are highter/lower than observed in the surrounding areas (Greatbatch *et al.*, 2004), and the continuing path of the Gulf Stream is innaccurate from the earlier misrepresentation. Given the importance of climate change and research into global warming, accurate representations of SSTs are vital for realistic predictions of the planets climate. Among the many processes at play are two gyres, the subpolar northern recirculation gyre (NRG) which lies to the North of the Gulf Stream, and the subtropical gyre to the south of the Gulf Stream. These two gyres contribute to the transport of the Gulf Stream (Hogg *et al.*, 1986), and can be seen to weaken, strengthen or be displaced in response to changing trends in many of the models used to investigate the Gulf Stream and it's related dynamics as in (Greatbatch, Fanning, and Goulding, 1991) and (Zhang and Vallis, 2007) among others.

1.2 Problems and Restrictions

Higher resolution models have been shown to provide a more realistic Gulf Stream path (Scaife *et al.*, 2011). However this comes at a cost requiring more processing power and thus a more expensive model. It is understood (Nikurashin, Vallis, and Adcroft, 2012) that this improvement is due to the higher resolution models being able to resolve small-scale processes which are lost in the coarser resolution counterparts. This is discussed further in section 2.
(Ezer, 2016) suggests that to replicate an accurate Gulf Stream separation, the model not only needs to resolve the Gulf stream but also the northern branches of NRG, the southward slope, and shelf currents. It is also thought that the lack

of detailed representation of the bathymetry in key areas plays a large role in the unrealistic Gulf Stream path. (Ezer, 2016) posed that it is the interaction with the bathymetry and the consequential small-scale processes which cause the Gulf Stream to split off from the coast at Cape Hatteras and direct it's path from there. The bathymetry itself can be represented in many different ways in the model and the vertical coordinate system chosen has a large impact on the interaction of the ocean dynamics and the ocean floor. We discuss this in more detail in section 3.

The Gulf Stream is ∼100km wide and varies from a depth of 800-1200km. Coarser models of 1°resolve to 100km per cell while 0.25°models resolve ∼25km per cell. These scales compared to the ∼100km width of the Gulf Stream demonstrate that a higher resolution model should give a clearer representation. This is akin to trying to identify a pixelated image - the higher the resolution, the clearer the picture.

2 The Dynamics of the Gulf Stream

The Gulf stream separates at Cape Hatteras, skirts the Grand Banks at Newfoundland and then heads Eastwards towards western Europe. However, in many moderate resolution climate models this separation occurs further north than observed and turns more sharply to the East, as noted in (Hurlburt and Hogan, 2008) and often misses off the Grand Banks, heading straight towards Europe. This can lead to what modellers refer to as the "blue spot of death" (Gnanadesikan, Griffies, and Samuels, 2007), a patch of colder than observed SSTs resulting from the lack of heat at Newfoundland normally brought up by the Gulf Stream.

The exact cause for the path of the Gulf Stream is unknown, though it has been a research topic for many years and is still a popular topic amongst researchers today. A recurring theme when looking into the separation of the Gulf Stream is the mention of bathymetry. It is thought (Gula, Molemaker, and McWilliams, 2014)(Naveira Garabato *et al.*, 2013)(Nikurashin, Vallis, and Adcroft, 2012) that the ocean dynamics resulting from the interaction of the Gulf Stream and the deep western boundary current (DWBC) with the bathymetry in the North Atlantic could cause the turbulence required to direct the Gulf Stream along its path. A sudden change in the direction of the Gulf Stream just off the coast at South

Carolina and Georgia has been attributed by (Gula, Molemaker, and McWilliams, 2014) to the Charleston Bump, a topographical feature which raises the ocean floor, from a depth of 600m on the surrounding Blake Plateua to 200m. Hence it is clear that bathymetry can strongly impact the direction of ocean currents.

2.1 The Effects of topography

(Naveira Garabato *et al.*, 2013) explain the dynamics of the ocean as a balance between the wind stress causing acceleration on the surface against the deceleration of the pressure forces resulting from the bathymetry. The extent of the impact of topography on ocean dynamics can be seen by examining the difference between flat bottom models and models with realistic bathymetry.

There are many ways to look into these differences, but we will focus mainly on two terms, the bottom pressure torque and the Joint Effect of Baroclinicity And Relief (JEBAR), as used by (Greatbatch, Fanning, and Goulding, 1991), (Bell, 1999), (Gula, Molemaker, and McWilliams, 2014) as well as many others.

2.1.1 The Joint Effect of Baroclinicity and Relief (JEBAR)

The JEBAR term was first introducted to account for the effects of topography and baroclinicity after the unrealistic results yielded from the more traditional flat-bottomed models. (Meyers, Fanning, and Weaver, 1996) states that this term is crucial for accurate Gulf Stream separation. The term arises from the barotropic vorticity equation after taking the curl of the vertically averaged zonal and meridional flow.

We will follow the derivation of the JEBAR and bottom pressure torque terms used in (Greatbatch, Fanning, and Goulding, 1991) as it shows the barotropic vorticity equation as a combination of a JEBAR term and a wind term, demonstrating the balance referenced by (Naveira Garabato *et al.*, 2013)

First we introduce the horizontal momentum equations (1) & (2), the hydrostatic relation (3) and the continuity equation (4) determining flow in spherical coordinates

$$-fv = -\frac{1}{a\rho_0 \cos\phi}\frac{\partial p}{\partial \lambda} + \frac{1}{\rho_0}\frac{\partial \tau_{z\lambda}}{\partial z} \tag{1}$$

$$fu = -\frac{1}{a\rho_0}\frac{\partial p}{\partial \phi} + \frac{1}{\rho_0}\frac{\partial \tau_{z\phi}}{\partial z} \tag{2}$$

$$0 = -\frac{\partial p}{\partial z} - \rho_0 b \tag{3}$$

$$\frac{1}{a\cos\phi}\left(\frac{\partial u}{\partial \lambda} + \frac{\partial}{\partial \phi}\left(v\cos\phi\right)\right) + \frac{\partial w}{\partial z} = 0 \tag{4}$$

taking the coordinates with λ as the longitude, ϕ as the latitude and z as the altitude from the sea surface ($z = 0$) upwards. The remaining terms are: u, v, and w are the zonal, meridional and vertical velocity; a is the Earth's radius; ρ_0 is the density of seawater; p is the pressure perturbation; $b = g\frac{(\rho-\rho_r)}{\rho_0}$ is the negative buoyancy (where $\rho_r = \rho_r(z)$, the horizontally averaged denisty at depth z, and g is the acceleration due to gravity); and $\tau_{z\lambda}$ and $\tau_{z\phi}$ are turbulent Reynolds stresses. In line with the (Greatbatch, Fanning, and Goulding, 1991) derivation we neglect the local time derivative, nonlinear advection and horizontal Reynolds stress as we are focused on the vertical integration of the equations.

First we introduce the notation

$$U = \int_{-H}^{0} u\,\mathrm{d}z, \quad V = \int_{-H}^{0} v\,\mathrm{d}z. \tag{5}$$

We now establish a streamfunction ψ satisfied by U and V by taking the vertical integral of (4)

$$\frac{1}{a\cos\phi}\left(\frac{\partial U}{\partial \lambda} + \frac{\partial}{\partial \phi}\left(V\cos\phi\right)\right) = 0. \tag{6}$$

We then have the define the required streamfunction by

$$aU = -\frac{\partial \psi}{\partial \phi}, \quad aV\cos\phi = \frac{\partial \psi}{\partial \lambda}. \tag{7}$$

Taking the vertical averages of (1) and (2) gives

$$-\frac{fV}{H} = -\frac{1}{Ha\rho_0\cos\phi}\int_{-H}^{0}\frac{\partial p}{\partial \lambda}\,\mathrm{d}z + \frac{1}{H\rho_0}\left[\tau_\lambda^s - \tau_\lambda^b\right] \tag{8}$$

$$\frac{fU}{H} = -\frac{1}{Ha\rho_0}\int_{-H}^{0}\frac{\partial p}{\partial \phi}\,\mathrm{d}z + \frac{1}{H\rho_0}\left[\tau_\phi^s - \tau_\phi^b\right] \tag{9}$$

where $\left(\tau_\lambda^s, \tau_\phi^s\right)$ and $\left(\tau_\lambda^b, \tau_\phi^b\right)$ are the surface wind stresses and bottom stresses respectively. Following (Greatbatch, Fanning, and Goulding, 1991) we take the bottom stress to be zero $\left(\tau_\lambda^b = \tau_\phi^b = 0\right)$.

Now we multiplying through by a and cross differentiating the vertically integrated momentum equations using

$$\frac{\partial}{\partial \lambda}(15) - \frac{\partial}{\partial \phi}(14)\cos\phi \tag{10}$$

and substituting for the streamfunction defined in (7) and the hydrostatic relation (3) for the pressure terms, yields

$$\frac{\partial \psi}{\partial \phi}\frac{\partial}{\partial \lambda}\left(\frac{f}{H}\right) - \frac{\partial \psi}{\partial \lambda}\frac{\partial}{\partial \phi}\left(\frac{f}{H}\right) = \frac{\partial}{\partial \phi}\frac{1}{H}\frac{\partial}{\partial \lambda}\left(\int_{-H}^{0} zb\,\mathrm{d}z\right) - \frac{\partial}{\partial \lambda}\frac{1}{H}\frac{\partial}{\partial \phi}\left(\int_{-H}^{0} zb\,\mathrm{d}z\right) + \frac{a}{\rho_0}\left[\frac{\partial}{\partial \lambda}\left(\frac{\tau_\phi^s}{H}\right) - \frac{\partial}{\partial \phi}\left(\frac{\tau_\lambda^s \cos\phi}{H}\right)\right]. \tag{11}$$

By letting

$$\Phi = \int_{-H}^{0} zb\,\mathrm{d}z \tag{12}$$

and using the Jacobian operator, we can separate (11) into three terms

$$J\left(\psi, \frac{f}{H}\right) = J\left(\Phi, \frac{1}{H}\right) + \frac{a}{\rho_0}\left[\frac{\partial}{\partial \lambda}\left(\frac{\tau_\phi^s}{H}\right) - \frac{\partial}{\partial \phi}\left(\frac{\tau_\lambda^s \cos\phi}{H}\right)\right] \tag{13}$$

resulting in the desired form. The term on the left hand side of the eqaution represents the transport across f/H contours, which is driven by the two terms on the right hand side. The first term on the right hand side of the equation is the JEBAR term and the second is the vorticity input from the wind.

This representation of the streamfunction driven by two separate forces has

lead researchers to split the streamfunction into separate parts to allow further investigation. (Greatbatch, Fanning, and Goulding, 1991) follow on from their derivation of the above terms to later separate ψ into three parts, one driven by the wind terms and two parts driven by the differnt aspects of the JEBAR term.

2.1.2 Bottom Pressure Torque

We arrive at the bottom pressure torque in similar way to JEBAR, however instead of taking the curl of the vertically averaged flow, we now take the curl of the vertically integrated zonal and meridional flow. Again we follow the derivation of (Greatbatch, Fanning, and Goulding, 1991).

Vertically integrate the momentum equations (1) and (2) over the depth of the water column to obtain HERE

$$-fV = -\frac{1}{a\rho_0 \cos\phi}\left[\frac{\partial}{\partial\lambda}\left(\int_{-H}^{0} p\,\mathrm{d}z\right) - p_b H_\lambda\right] + \frac{1}{\rho_0}\left(\tau_\lambda^s - \tau_\lambda^b\right) \tag{14}$$

$$fU = -\frac{1}{a\rho_0}\left[\frac{\partial}{\partial\phi}\left(\int_{-H}^{0} p\,\mathrm{d}z\right) - p_b H_\phi\right] + \frac{1}{\rho_0}\left(\tau_\phi^s - \tau_\phi^b\right) \tag{15}$$

where p_b is the bottom pressure and we take $\tau_\lambda^b = \tau_\phi^b = 0$ as before.
Multiplying through by a, cross differentiating (taking the curl) of (14) and (15) as in (10), using (6) and substituting for the streamfunction defined in (7), yields

$$\left(\frac{\mathrm{d}f}{\mathrm{d}\phi}\right)\frac{\partial\psi}{\partial\lambda} = \frac{1}{\rho_0}\left(-\frac{\partial p_b}{\partial\phi}\frac{\partial H}{\partial\lambda} + \frac{\partial p_b}{\partial\lambda}\frac{\partial H}{\partial\phi}\right) + \frac{a}{\rho_0}\left[\frac{\partial}{\partial\lambda}\left(\tau_\phi^s\right) - \frac{\partial}{\partial\phi}\left(\tau_\lambda^s\cos\phi\right)\right]. \tag{16}$$

The first term on the right hand side of this equation corresponds to the bottom pressure torque and can be represented using the Jacobian as

$$J(p_b, H) = -\frac{\partial p_b}{\partial\phi}\frac{\partial H}{\partial\lambda} + \frac{\partial p_b}{\partial\lambda}\frac{\partial H}{\partial\phi}. \tag{17}$$

The second term on the right hand side of (16) is the surface wind stress.

(Greatbatch, Fanning, and Goulding, 1991) show that if the bottom pressure torque in term in (16) is 0, we are left with the flat-bottomed Sverdrup relation.

Thus the bottom pressure torque term accounts for the effects of the bottom topography on the flow. (Greatbatch, Fanning, and Goulding, 1991) go on to separate the the streamfunction into two parts, one driven by the bottom pressure torque and the other driven by the flat-bottomed Sverdrup relation.

The impact of the bottom topography is demonstrated well by examining Figure 1, comparing three figures from (Greatbatch, Fanning, and Goulding, 1991). 1 shows the total streamfunction in a) and then decomposed into the case of no topography, driven only by the flat-bottomed Sverdrup relation in b), and the contribution from the bottom pressure torque term in c). It is evident that although the result is a combination of the terms, there is a significant impact on the transport by the twisting forces resulting from the bottom pressure torque, especially in areas key for the Gulf Stream (such as the area around the Grand Banks).

The bottom pressure torque is important for the separation of the Gulf Stream as (Zhang and Vallis, 2007) shoed that the effect of bottom pressure torque with the DWBC has a strong impact on the NRG and thus the dynamics affecting the Gulf Stream.

2.2 Small Scale Processes

It has been noted that in higher resolution models, the separation and subsequent path of the Gulf Stream is much more accurate than in the lower resolution counterparts (Hurlburt and Hogan, 2008)(Zhang and Vallis, 2007). This lends to the idea that the processes which affect the Gulf Stream occur on smaller scales which aren't resolved by coarser models (Naveira Garabato *et al.*, 2013)(Nikurashin, Vallis, and Adcroft, 2012). Various processes have been investigated and suggested as the main influences though it is likely that the improved Gulf Stream representation is due to multiple factors.

(Naveira Garabato *et al.*, 2013) theorised that interaction with the bathymetry creates small-scale turbulence and instabilities which could cause bathymetric steering and divert currents. If this is not being represented in coarser models, the energy behind the turbulence must be going elsewhere. (Scott *et al.*, 2010) compared current meter readings with modelled values for kinetic energy and noticed that in some areas of the North Atlantic the total kinetic energy was being

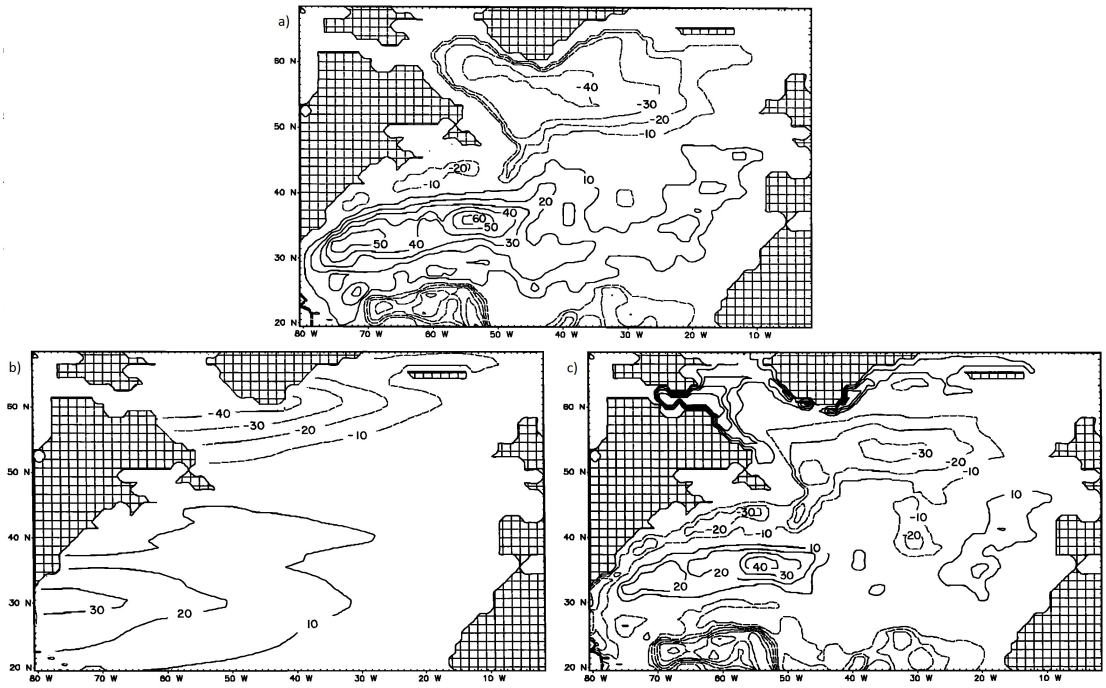

Figure 1: a) The Transport stream function (annual mean field) calculated using climatological mean wind density data. The contour interval is 10Sv. Dashed contours indicate negative values; solid contours, positive values. b) As a) but for a flat-bottomed ocean. c) As a) but showing only the contributions from the bottom pressure torque (Figs. 1, 5 and 6 from (Greatbatch, Fanning, and Goulding, 1991))

held higher in models than observed. It is discrepancies such as this which could have much wider implications. If the energy is not penetrating to the ocean floor, we cannot expect to be able to replicate the effects of the bathymetry. Perhaps by pulling this energy further down (closer to observed values), there would be more energy transfer from the larger ocean eddies to the smaller scale turbulence resulting from interaction with the bathymetry.

(Tansley and Marshall, 2001) used a simplified model of water flowing past a cylinder to highlight the importance of turbulence on fluid motion. Using a quarter-cylinder (mimicking a simplified version of Cape Hatteras) and a high Reynolds number (allowing for more turbulent flow), the model produced a jet with surrounding turbulent eddies similar to those observed in the Gulf Stream

. These results were not seen with a lower Reynolds number, highlighting the importance of turbulence in forming jets like the Gulf Stream.

The turbulent mixing arising from interaction with the bathymetry could allow geostrophic eddies to transfer some of their energy to smaller processes by causing internal waves to break and contribute to enhanced mixing (Nikurashin, Vallis, and Adcroft, 2012). These effects have been seen even in cases of small-scale bathymetric roughness suggesting that it is not necessary to have large topological features to impact ocean dynamics, instead small surface differences can cause changes which lead to bigger outcomes.

(Naveira Garabato *et al.*, 2013) attribute the significant impact of small-scale bathymetry to wave drag. Although wave drag is not a large contributor to ocean dynamics, topological features on a small scales can cause wave drag which contributes ten to several tens of a percentage of the dominant source and sink terms influencing the vorticity of the ocean.

These effects of small-scale processes are not limited to the Gulf Stream, but impact on many aspects of ocean dynamics as the various currents and features affect one another. (Ezer, 2016) speculated that amongst other things, the northern branches of the Northern Recirculation Gyre (NRG) would have to be resolved in order to produce an accurate Gulf Stream in a model. (Zhang and Vallis, 2007) determined that a significant contribution to the generation of the NRG is the bottom vortex stretching resulting from a downslope DWBC, which is in turn the result of the interaction with bathymetry as the DWBC crosses the path of the Gulf Stream. Hence, bathymetric impact can circle around to affect many aspects of ocean dynamics.

3 Modelling the Gulf Stream

As more scientists seek to understand ocean dynamics, more models are made and used by different researchers to simulate different processes. There are many models in use today, all with different configurations and settings. This can lead to contrasting outcomes and debate over which choice of model or model settings yields the most accurate results.

3.1 Model Resolution

Along with differing numerical schemes or boundary conditions, etc. there are also many different model resolutions available. These range from coarse 1° models, which resolve to a scale of ≈ 100km, to higher resolution 0.25° models, which resolve to a scale of ≈ 25km, all with varying numbers of vertical levels. It is well established (Scaife *et al.*, 2011)(Hurlburt and Hogan, 2008) that a higher resolution ocean model tends to produce a more accurately resolved Gulf Stream. This is in part due to the small scale processes, mentioned previously, which contribute to the ocean circulation, but are not resolved in the coarser models. Unfortunately higher resolution models require additional processing power and thus additional costs. This means that the high resolutions required to resolve a realistic Gulf Stream will not be widely used for some time. Hence, the aim is to find a way to represent an accurate Gulf Stream in the lower resolution models by understanding the reasons behind it.

3.2 Vertical Coordinate System

One of the main variabilities between different models is the handling of the vertical coordinate system. The way in which the model splits the depth of the ocean into 'levels' can have a large impact on the way the bathymetry is represented. As previously discussed, this bathymetric representation can have large impacts on the dynamics within the model. The importance and significance of the bathymetric roughness has already been discussed in this review so it is now necessary to discuss the different ways to represent this.

The main coordinate systems in use are the z-coordinate system which stays true to a cartesian system of coordinates, consisting of rectangular 'blocks', which create a staircase effect when representing slopes. These z-coordinate systems can also be implemented with 'partial cells' whereby some of the cells are cut into smaller cells to 'smooth out' and more closely represent the shape of the slopes. Thre are also s- (or sigma-) coordinates which follow the shape of the terrain. The depth at any point is divided by the number of levels to create a consistent number of cells at all points of different thickness. These different approaches can also be combined to form hybrid coordinate systems. See Figure 2 for an illustration of

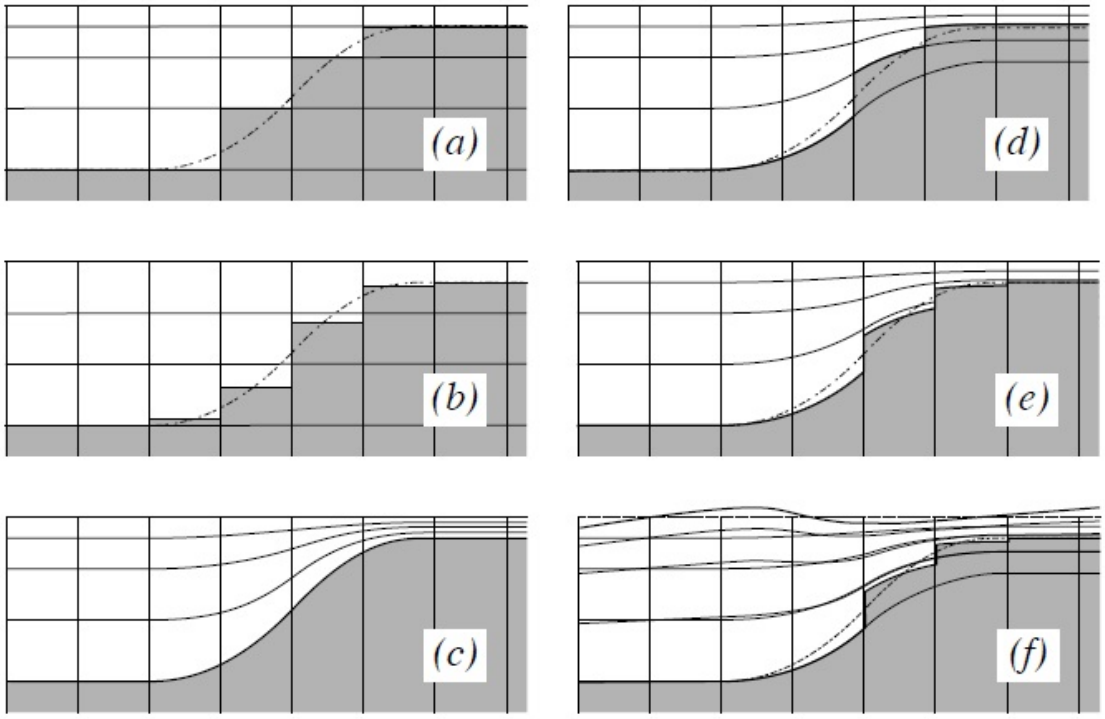

Figure 2: An illustration of different veritcal coordinate systems available in NEMO. (Madec, 2011). (a) z-coordinate, (b) z-coordinate with partial cells, (c) s-coordinate, (d) hybrid s-z coordinate, (e) hybrid s-z coordinate with partial cell, (f) shows (e) with a non-linear free surface (which can be used with any coordinate system).

some of the possible vertical coordinate systems available in the NEMO model.

The main difficulty in comparing different vertical coordinate systems lies in the availability of a 'control' case for the comparison. With the wide selection of models available to researchers, it is not only the vertical coordinate system which differs but also the numerical schemes being used to resolve various processes. This could lead to false similarities or differences and cause incorrect conclusions. (Ezer, 2016) was able to compare results from z-coordinate models and s-coordinate models while minimalising any other differnces between the models. Although the z-coordinate models are capable of producing an accurate Gulf Stream at hight resolutions, the s-coordinate models provided a more accurate representation when restricted with coarser models. However, as (Ezer, 2016) noted in the comparison, partial and shaved cells (whereby corners of the cells are 'shaved' off to smooth

out slopes) were not used in any of these models.

4 Barotropic Vorticity Diagnostics

Using the NEMO model, we are in the process of calculating barotropic vorticity diagnostics to further investigate the processes effecting the path of the Gulf Stream. These barotropic vorticity diagnostics have been used by (Bell, 1999), (Gula, Molemaker, and McWilliams, 2014) and (Yeager, 2015) among others, to investigate the driving forces behind the vorticity budgets in the North Atlantic.

Two different diagnositcs will be calculated on each of the seven contributing terms to the momentum equations shown in equation (18). The methods are similar to the approach taken in section (2.1) to find the JEBAR and bottom pressure torque terms and involve taking the curl of the vertically averaged and vertically integrated contributions.

Examining and comparing the results will help to highlight the leading terms driving the flow in different regions of the Gulf Stream. This may highlight key areas of bathymetry or emphasise the importance of the interaction with the DWBC.

4.1 NEMO Ocean Model

As the Barotropic Vorticity Diagnostics are being implemented in the NEMO model, it seems sensible to first introduce the model in a little more detail.
The Nucleus for European Modelling of the Ocean (NEMO) is a framework designed to allow for a flexible study of the ocean, it's dynamics and it's interaction with other climate systems (Madec, 2011).

The framework of NEMO allows the model to be configured in a variety of ways, choosing the resolution, numerical schemes and vertical coordinates according to your requirements. As discussed in section 3, the representation of the Gulf Stream can vary greatly depending on various aspects of the model chosen. The resolution can play a big role as discussed in (Scaife *et al.*, 2011), and (Ezer, 2016)

showed that path of the Gulf Stream is sensitive also to the choice of vertical coordinates and bathymetrical representation. It is suitable then, for our requirements, as it will allow comparisons between a variety of different configurations in a way which can be problematic for most modellers (as noted in (Ezer, 2016)).

Within NEMO are many different engines designed to model different aspects of the ocean, these are OPA, which models the ocean dynamics and thermodynamics; LIM, which models the sea-ice dynamics and thermodynamics; and Top, modelling the biogeochemistry. For our purposes we are interested in OPA, which will we will run off the MONSooN super computer.
We can further narrow our interests for the current investigation within OPA down to the routines focusing on the ocean dynamics. This part of the model is located within the DYN directory of the code and is responsible for the momentum equations, which are key to the barotropic vorticity diagnostics and are the focus of this section.

The prognostic Prognostic Ocean dynamics equations used by NEMO (where (NXT) stands for the next time step) are

$$NXT = \underbrace{(VOR + KEG + ZAD)}_{\text{Coriolis \& advection}} + \underbrace{HPG + SPG}_{\text{Pressure gradient contributions}} + \underbrace{LDF}_{\text{lateral diffusion}} + \underbrace{ZDF}_{\text{vertical diffusion}} . \tag{18}$$

Here the Coriolis and advection terms are split into three parts: the vorticity (VOR), the kinetic enery (KEG) and the vertical advection (ZAD). In place of the Coriolis and advection terms shown here, in the flux formation, they can be replaced by a coriolis and advection term $(COR + ADV)$, however, for our purposes we wil be using the terms shown in equation (18). The pressure gradient contributions consist of the hydrostatic pressure gradient (HPG) and the surface pressure gradient (SPG), and we also have the lateral (LDF) and vertical diffusion (ZDF) terms (Madec, 2011).

Currently the diagnostics are being added to a 0.25° model using the z-coordinate bathymetry with partial setps (shown in Figure 2 (b)). Following the successful

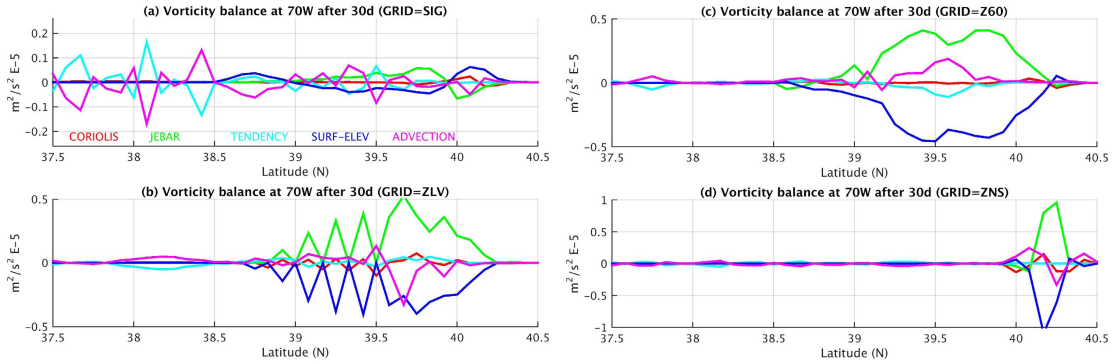

Figure 3: Leading terms of the vorticity balance equation at 70°W after 30 days for experiments: (a) SIG (sigma coordinates), (b) ZLV (z-level coordinates with 21 layers), (c) Z60 (z-level coordinates with 61 layers) and (d) ZNS (z-level coordinates with no continental slope). Note the different scale in each panel. Each term has different color as indicated in (a). (Fig. 8 from (Ezer, 2016)) An example of the kind of results available from barotropic vorticity diagnostics.

implementation of these diagnostics in one model formulation in NEMO, the intention is to then compare the results gained from running the calculations across different model resolutions and possibly different choices of vertical coordinates.

This could build on the review by (Ezer, 2016) by allowing for a more controlled comparison between models and allow an easier comparison and analysis of the results. Figure 3 (Fig. 8 from (Ezer, 2016)) shows the effect that the choice of model grid can have on the balance of the barotropic vorticity budget. With the various available configuration of NEMO, it will be interesting to further investigate this within a more controlled set up.

4.2 Barotropic Vorticity Diagnostics

New code has been added to the NEMO model to calculate the two diagnostics. As each contribution to the momentum trend is calculated, it is passed to the subroutine which then calculates the required values.

The subroutine first calculates the vertical integral of the contribution, $\bar{u}$ and $\bar{v}$, over the height of the water column from the depth, $-H$, to the sea surface level η,

$$\bar{u} = \int_{-h}^{\eta} u \, \mathrm{d}z \,, \quad \bar{v} = \int_{-h}^{\eta} v \, \mathrm{d}z \tag{19}$$

and then divide through by the height of the water column to obtain the vertical averages $\langle \bar{u} \rangle$ and $\langle \bar{v} \rangle$,

$$\langle \bar{u} \rangle = \frac{1}{\eta + h} \int_{-h}^{\eta} u \, \mathrm{d}z \,, \qquad \langle \bar{v} \rangle = \frac{1}{\eta + h} \int_{-h}^{\eta} v \, \mathrm{d}z. \tag{20}$$

We now take the curl of each of these values to attain the two desired diagnostics

$$\Omega = \frac{\partial \bar{v}}{\partial x} - \frac{\partial \bar{u}}{\partial y} \tag{21}$$

$$\Omega_{avg} = \frac{\partial \langle \bar{v} \rangle}{\partial x} - \frac{\partial \langle \bar{u} \rangle}{\partial y}. \tag{22}$$

Once the diagnostics have been calculated we can then compare the different contributions as in (Yeager, 2015) and (Gula, Molemaker, and McWilliams, 2014). Using equation (7) we can also calculate the barotropic streamfunction driving the flow.

5 Future Work

We have now established the importance of a robust and accurately modelled Gulf Stream, however the path to achieving this is not yet clear. We seek to improve the understanding and thus the representation of the Gulf Stream in moderate resolution models. As discussed, there are many processes involved in the dynamics of the ocean and thus there are many different directions to turn to when seeking solutions to this problem. Here we will focus on the interactions and effects of the bathymetry while being careful not to ignore other paths this investigation may lead down.

5.1 Identifying key processes

The barotripic vorticity diagnostics currently being persued may lead to some intersting findings into the vorticity balances in different model resolutions and configurations. With this insight, we can hope to identify some key areas or

processes which could explain the improvements in the representation of the Gulf Stream seen by (Scaife *et al.*, 2011) and others when increasing model resolution.

5.2 Different model formulations

The many different ocean and OGCM models available allow us to see the effects of many different schemes and parameterisations in use today. In particular the choice of vertical coordinate system has long been discussed, especially in regard to its relevance here. Obviously the representation of the topography and the way it is rendered in the model is a result of the vertical coordinate choice. (Ezer, 2016) revisited the discussion in relation to the Gulf Stream separation and used similar models to determine the most accurate results over different choices for coordinate systems. However, the z-coordinate system chosen did not include any partial or shaved cells. It is clear that using the z-coordinate system would cause the various slopes in the ocean floor to appear as 'steps' which would significantly alter the flow around the area. It is not so surprising perhaps that under these circumstances (Ezer, 2016) found sigma or s-coordinates to be the most realistic given that they allow for a smooth ocean floor. It is perhaps natural then to question the effect of partial or shaved cells on these findings. As NEMO allows for such a diverse range of configurations and schemes, it would be interesting to recreate these results while implementing a z-coordinate system with partial cells to allow for a new take on this review. Indeed that has already been mentioned as a possible extension of the barotropic vorticity diagnostics discussed in section 4.

As discussed previously and shown by (Zhang and Vallis, 2007) and others, the NRG and subtropical gyres either side of the Gulf Stream can have significant effects on the path on the Gulf Stream itself, as well as contributing to the strength of it's transport. To further examine the interplay between the NRG and the path of the Gulf Stream, a simple configuration of NEMO simulating the double gyre seen in the North Atlantic could be used to examine the dynamics in an idealised model. This could be investigated using the barotropic vorticity diagnostic or by other means. In (Zhang and Vallis, 2007) it was clear that the correct viscosity was required to attain a realistically-strong gyre, demonstrating that there are various

factors to be examined when trying to explain the dynamics. Results from this could help to influence analysis within the more realistic models. As (Tansley and Marshall, 2001) used the classic problem of flow past a cylinder to understand the Gulf Stream separation, we too can learn from idealised set up and by breaking the problem down to its fundamental aspects.

5.3 Understanding the Gulf Stream

It has been discussed in section 2 that a lack of energy transfer, either by lack of interaction with the bathymetry, or via some other process, could be to blame for the low levels of turbulence found in the area surrounding the separation of the Gulf Stream. This is an area which has seen less investigation. Examining the reason for the lack of depth penetration could be an interesting route to go down, though one which requires more thought into how.

The evolution of the Gulf Stream is of keen interest for climate models. The change of 30Sv between the pentads 1955-59 and 1970-74 discussed by (Greatbatch, Fanning, and Goulding, 1991) is understood to be due to a dramatic change in strength of the subtropical gyre. However, global warming brings the threat of a slowdown (or shutdown) of the thermohaline circulation (Gough and Allakhverdova, 1998). It is then important that we are able to understand the longer-term evolution of the Gulf Stream and what drives the changes prompting it. This could be investigated using some longer time integrations to gain insight into the overarching adjustments in the dynamics of the North Atlantic. Again this requires more thought but could provide some interesting results.

The search for better comprehension of the dynamics involved in the global ocean dynamics could lead in many directions. Ulitmately it is only through improved understanding that we can improve the representation of the Gulf Stream in moderate resolution climate models.

References

Bell, M.J.: 1999, Vortex stretching and bottom torques in the Bryan-Cox ocean circulation model. *Journal of Geophysical Research* **104**, 265 – 286.

Ezer, T.: 2015, Detecting changes in the transport of the Gulf Stream and the Atlantic overturning circulation from coastal sea level data: The extreme decline in 2009-2010 and estimated variations for 1935-2012. *Global and Planetary Change* **129**, 23 – 36. doi:10.1016/j.gloplacha.2015.03.002. http://dx.doi.org/10.1016/j.gloplacha.2015.03.002.

Ezer, T.: 2016, Revisiting the problem of the Gulf Stream separation: On the representation of topography in ocean models with different types of vertical grids. *Ocean Modelling* **104**, 15 – 27. doi:10.1016/j.ocemod.2016.05.008.

Gnanadesikan, A., Griffies, S.M., Samuels, B.L.: 2007, Effects in a climate model of slope tapering in neutral physics schemes. *Ocean Modelling* **16**(1-2), 1 – 16. ISBN 1463-5003. doi:10.1016/j.ocemod.2006.06.004.

Gough, W.A., Allakhverdova, T.: 1998, Sensitivity of a coarse resolution ocean general circulation model under climate change forcing. *Tellus* **50**(A), 124 – 133.

Greatbatch, R.J., Fanning, A.F., Goulding, A.D.: 1991, A Diagnosis of Interpentadal Circulation Changes in the North Atlantic. *JOURNAL OF GEOPHYSICAL RESEARCH* **96023**(15), 9 – 22. doi:10.1029/91JC02423.

Greatbatch, R.J., Sheng, J., Eden, C., Tang, L., Zhai, X., Zhao, J.: 2004, The semi-prognostic method. *Continental Shelf Research* **24**(18), 2149 – 2165. doi:10.1016/j.csr.2004.07.009.

Gula, J., Molemaker, M.J., McWilliams, J.C.: 2014, Gulf Stream Dynamics along the Southeastern U.S. Seaboard. *Journal of Physical Oceanography* **45**(3), 690 – 715. doi:10.1175/JPO-D-14-0154.1. http://journals.ametsoc.org/doi/abs/10.1175/JPO-D-14-0154.1%5Cnhttp://journals.ametsoc.org/doi/pdf/10.1175/JPO-D-14-0154.1.

Hogg, N.G., Pickart, R.S., Hendry, R.M., Smethie, W.J.: 1986, The northern recirculation gyre of the gulf Stream. *Deep Sea Research Part A, Oceanographic Research Papers* **33**(9), 1139 – 1165. doi:10.1016/0198-0149(86)90017-8.

Hurlburt H.E., Hogan P.J.: 2008, The Gulf Stream pathway and the impacts of the eddy-driven abyssal circulation and the Deep Western Bound-

ary Current. Dynamics of Atmospheres and Oceans. ISBN 0377-0265. doi:10.1016/j.dynatmoce.2008.06.002.

Madec G.: 2011, NEMO Ocean Engine, 1 – 332. http://www.nemo-ocean.eu/About-NEMO/Reference-manuals{%}5Cnpapers2://publication/uuid/73E7FF17-99BE-4B10-A823-0037C823EF6E.

Meyers P.G., Fanning A.F., Weaver A.: 1996, JEBAR, bottom pressure torque and Gulf Stream separation. doi:10.1175/1520-0485(1996)026¡0671:JBPTAG¿2.0.CO;2.

Naveira Garabato, A.C., Nurser, A.J.G., Scott, R.B., Goff, J.A.: 2013, The Impact of Small-Scale Topography on the Dynamical Balance of the Ocean. *Journal of Physical Oceanography* **43**(3), 647 – 668. doi:10.1175/JPO-D-12-056.1. http://journals.ametsoc.org/doi/abs/10.1175/JPO-D-12-056.1.

Nikurashin, M., Vallis, G.K., Adcroft, A.: 2012, Routes to energy dissipation for geostrophic flows in the Southern Ocean. *Nature Geoscience* **6**(1), 48 – 51. ISBN 1752-0894. doi:10.1038/ngeo1657. http://www.nature.com/doifinder/10.1038/ngeo1657.

Scaife A.A., Copsey D., Gordon C., Harris C., Hinton T., Keeley S., O'Neill A., Roberts M., Williams K.: 2011, Improved Atlantic winter blocking in a climate model. Geophysical Research Letters. ISBN 0094-8276. doi:10.1029/2011GL049573. http://0-onlinelibrary.wiley.com.lib.exeter.ac.uk/doi/10.1029/2011GL049573/epdf.

Scott, R.B., Arbic, B.K., Chassignet, E.P., Coward, A.C., Maltrud, M., Merryfield, W.J., Srinivasan, A., Varghese, A.: 2010, Total kinetic energy in four global eddying ocean circulation models and over 5000 current meter records. *Ocean Modelling* **32**(3-4), 157 – 169. ISBN 1463-5003. doi:10.1016/j.ocemod.2010.01.005. http://dx.doi.org/10.1016/j.ocemod.2010.01.005.

Tansley, C.E., Marshall, D.P.: 2001, Flow past a Cylinder on ab Plane, with Application to Gulf Stream Separation and the Antarctic Circumpolar Cur-

rent. *Journal of Physical Oceanography* **31**, 3274 – 3284. doi:10.1175/1520-0485(2001)031¡3274:FPACOA¿2.0.CO;2.

Yeager, S.: 2015, Topographic Coupling of the Atlantic Overturning and Gyre Circulations. *Journal of Physical Oceanography* **45**(5), 1258 – 1284. doi:10.1175/JPO-D-14-0100.1. http://dx.doi.org/10.1175/JPO-D-14-0100.1.

Zhang, R., Vallis, G.K.: 2007, The Role of Bottom Vortex Stretching on the Path of the North Atlantic Western Boundary Current and on the Northern Recirculation Gyre. *Journal of Physical Oceanography* **37**, 2053 – 2080. doi:10.1175/JPO3102.1.